Arabian Journal of Chemistry (2021) **14**, 103293

King Saud University

Arabian Journal of Chemistry

www.ksu.edu.sa
www.sciencedirect.com

ORIGINAL ARTICLE

Anti-arthritic activity of Tin oxide-Chitosan-Polyethylene glycol carvacrol nanoparticles against Freund's adjuvant induced arthritic rat model via the inhibition of cyclooxygenase 2 and prostaglandin E2

Zhao Tian [a,*], Arunachalam Chinnathambi [b], Tahani Awad Alahmadi [c], Surapaneni Krishna Mohan [d], Vishnu Priya Veeraraghavan [e], Saravana Kumar Jaganathan [f]

[a] *Department of Orthopedics, The First Affiliated Hospital of Xi' an Jiaotong University, 277 West Yanta Road, Xi'an, Shaanxi, 710061, People' s Republic of China*
[b] *Department of Botany and Microbiology, College of Science, King Saud University, PO Box-2455, Riyadh 11451, Saudi Arabia*
[c] *Department of Pediatrics, College of Medicine and King Khalid University Hospital, King Saud University, Medical City, PO Box-2925, Riyadh 11461, Saudi Arabia*
[d] *Department of Biochemistry, Panimalar Medical College Hospital & Research Institute, Varadharajapuram, Poonamallee, Chennai 600 123, India*
[e] *Department of Biochemistry, Saveetha Dental College, Saveetha Institute of Medical and Technical Sciences, Saveetha University, Chennai 600 077, India*
[f] *Department of Engineering, Faculty of Science and Engineering, University of Hull, Hu67RX, United Kingdom*

Received 21 April 2021; accepted 24 June 2021
Available online 30 June 2021

KEYWORDS

SCP-CAR nanocomposites;
Arthritis;
Inflammation;
Antioxidant

Abstract Rheumatoid arthritis (RA) results in increased rate of mortality in millions of people worldwide. Research utilizing Tin oxide – Chitosan- Polyethylene glycol Carvacrol (SCP-CAR) nanocomposites has gained increased attention because of its multipotent properties and application in diverse fields including medicinal preparations. The aim of the investigation was to synthesize and to examine the anti-arthritic ability of SCP-CAR nanocomposites against CFA -induced RA in rats. Arthritis induction was done by injecting 0.1 ml of Complete Freund's adjuvant (CFA) intradermally. Body

* Corresponding author.
E-mail address: tianzhaosuide@sina.com (Z. Tian).
Peer review under responsibility of King Saud University.

Production and hosting by Elsevier

https://doi.org/10.1016/j.arabjc.2021.103293

weight, weight of organs, hind paw volumes and arthritis score was assessed and the levels of inflammatory modulators such as IL-6, IL-1β, IL-10, TNF-α, PGE2 and COX-2 was examined using assay kits. Lipid peroxidation status, antioxidant enzyme activities and levels of liver function enzymes were evaluated using standard procedures. Histopathological changes observed in hind limb of experimental animals were viewed under microscope using H& E staining. The SCP-CAR nanocomposites treated arthritic animals showed increased bodyweight and reduced hind paw volume, organ weight and arthritis score together with elevated antioxidants status and depleted proinflammatory cytokines. Histopathological observation also showed reduction in bone destruction and penetration of inflammatory cells following treatment with SCP-CAR nanocomposites. Thus, together the findings depict the anti-arthritic and anti-inflammatory potential of SCP-CAR nanocomposites suggesting that it could be used as potent therapeutic agent to treat animals against arthritis induced by CFA.

1. Introduction

Rheumatoid arthritis (RA), an autoimmune disease affects millions of peoples around the world, results in increased rate of disability particularly among the age group of 30–50. It is characterized by joint inflammation, restriction of motor actions, destruction of articular cartilage and collapse the action of synovial joints finally resulting in disabilities that are irreversible (Grygielska et al., 2018). Progression of RA is closely associated with immune related pathological abnormalities. Most noticeable changes observed during the progression of RA include joint swelling, hyperplasia of synovial joints, formation of pannus, synovial membrane inflammation and stiffness of joints. Synovial intimal cells are the prime cells that participate in the processes of inflammatory reactions that are involved in RA progression (Okada et al., 2019).

Modulators of inflammation such as interleukin (IL)-1 and tumor necrosis factor- α (TNF-α) are generated through the activation of macrophages and neutrophils that aggravates inflammatory processes of RA (Dai et al., 2018). It is distinguished as progressive rheumatic inflammatory disorder that promotes inflammation and destruction of synovial membrane and bones of the joint (Pan et al., 2017). Activation of inflammatory cells was promoted in the synovial membrane through increased accumulation of pro-inflammatory mediators that are responsible for enhanced bone damage (Furst and Emery, 2014). In the pathological processes of RA, various crucial mediators are involved in severing the inflammatory mechanisms that include prostaglandin-E2 (PGE2), increased reactive oxygen species (ROS) generation and upregulated action of TNF-α, IL-1β and IL-6 that results in destruction of bones and cartilages, release of leukocyte and deteriorated activities of antioxidant enzymes. IL-4 and IL-10 are anti-inflammatory mediators, which decrease the inflammatory reactions provoked by pro-inflammatory cytokines. Inconsistency that occurs during RA between pro-inflammatory and anti-inflammatory molecules is regarded as accelerator of chronic inflammation (El-Gaphar et al., 2018).

Complete Freund's adjuvant (CFA) stimulated RA seen in experimental animals displayed similar features of RA noticed in humans and such model of RA was found to exert immediate response to inflammation (Bihani et al., 2014). Non-steroidal, steroidal and immunosuppressive drugs are available currently to treat RA that can reduce the swelling and joint pain even at lower dosage (McInnes and Schett, 2017).

Nanoparticles are helpful for delivering therapeutic drugs to the target cells and tissues and it is also considered to be safe and effective, as well as provide increased bioavailability of therapeutic drugs (Ulbrich and Lamprecht, 2010). Nanoparticles loaded drug delivery system has major advantages than traditional medicines since it has improved drug delivery, selective identification of specific target sites, minimal side effects, increased shelf life of drugs, effective release and transport together makes it as an effective prognostic material (Serra and Santamaria, 2015). Nanoparticles are found to be effective in drug delivery and its potency was reported in treating numerous diseases (Pham, 2011). Toxic side effects caused by chemotherapeutic agents can be minimized by nanoparticles and it improves their anti-inflammatory ability. Inflammatory cells as well as normal cells are subjected to toxicity by use of drugs which have anti-inflammatory efficacy. Incorporating nanoparticles into those anti-inflammatory drugs can increase their specificity and action on the target cells and tissues (Kapoor et al., 2014; Yang et al., 2017).

Size of nanoparticles are considered as the essential factor to understand the effectiveness and their efficacy may be improved through numerous approaches that include sonochemical, precipitation using chemicals, solgel and formulation prepared using plant extracts (Ruiz et al., 2015; Safa et al., 2016). Research utilizing nanoparticles from metals has gained increased attention because of its multipotent properties and application in diverse fields including medicinal preparations (Khashan et al., 2016). Nanoparticles synthesized using, metal oxides were predicted to have disinfecting action and therefore it is used in medical locations, as antimicrobial agents and also in cosmetics. These particles have excellent conducting ability that increases their demand in making medical instruments (Katwal et al., 2015).

Recently chitosan based nanocomposites received greater research interest due to its exceptional properties like biodegradability and biocompatibility, capacity to be sterilized by any techniques without reducing its properties, with many biological actions (Kumar et al., 2004; Singh and Ray, 2000; Ong et al., 2008). Carvacrol is a monoterpene phenolic compound found in many plant species (Lee et al., 2017). It was already reported that carvacrol exhibited many biological activities like anti-oxidant and anticancer (Baranauskaite et al., 2017), anti-inflammatory (Barnwal et al., 2017), anti-pyretic and analgesic (Singh et al., 2016) activities. However, the anti-inflammatory and antiarthritic activities of chitosan based carvacrol nanocomposites were not studied yet. Hence, the present study was proposed to prepare SCP-CAR nanoparticle composites and to understand its potent anti-inflammatory and anti-arthritic action against CFA-induced RA in rats.

2. Methods

2.1. Chemicals

All the chemicals and reagents utilized for the present analysis are of diagnostic grade and were procured from Sigma Aldrich, USA. Copper oxide, Complete Freund's adjuvant and the assay kits were purchased from Sigma Aldrich USA and MyBiosource, USA.

2.2. SCP-CAR (Tin oxide-Chitosan-Polyethylene glycol-Carvacrol) preparation

Tin oxide- Chitosan- Polyethylene glycol-Carvacrol nanocomposites were prepared as follows: 0.3 g of tin oxide (SnO2) NPs

was added to 20 ml of chitosan solution, and then SnO2-chitosan solution mixture was added into 20 ml of Polyethylene Glycol (PEG). Finally, the whole SnO2-Chitosan-PEG homogenizes mixture solution was added with 50 μL of Carvacrol solution. The SCP-Car nanocomposites were stirred continuously at 80 °C for 6 h. A white precipitate was formed on continuous stirring; the residue was centrifuged at 15000 rpm for 15 min at −4 °C. The solid SCP-CAR precipitate was washed several times with de-ionized water. Finally, the SCP-CAR nanocomposite was dried at 200 °C for 3 h.

2.3. Characterization studies

X-ray diffraction (XRD) pattern of SCP-CAR nanoparticle composites was observed by X-ray diffractometer using radiation of Cu Kα at wavelength of $\lambda = 0.1541$ nm which was represented in the scan range of 2θ angle ranging from 20° to 90°.

The nanocomposites from SCP-CAR were mixed with dry potassium bromide (KBr pellet) and subjected to a pressure of about 5×10 Pa in an evacuated die to produce a clear transparent disc of diameter 2 cm and thickness 0.2 cm. IR spectra in frequency region 4000–400 cm^{-1}, were recorded at room temperature on a Perkin Elmer Fourier transform infra-red (FTIR) spectrometer. Morphology and surface texture of SCP-CAR nanoparticle composites were studied using field emission scanning electron microscopy (FESEM). For size measurement, the nanoparticle composites were prepared using distilled water and then the size (Z-average mean) of the nanoparticles was analyzed by dynamic light scattering (DLS), using a Zetasizer ZS (Malvern Instruments, U.K). Absorption spectra of SCP-CAR nanocomposites dispersed in distilled water were measured using a UV–VIS spectrophotometer and the photoluminescence (PL) spectrum analysis of nanocomposites was measured by spectrofluorimeter (Hitachi, F-2500 FL).

2.4. Animal procurement

Male Wistar albino rats of about 200–250 g weight were procured from Institutional animal house facility and placed in polypropylene cages under standard laboratory conditions. The rats were fed with normal pellet diet and free access to water. Experiments were carried out based on the procedures issued by Institutional Animal ethical committee.

2.5. Experimental design

The rats used for the investigation were distributed randomly into four groups with six animals in all groups. Group I rats were considered as control animals administered with DMSO orally. Group II animals were considered as arthritis induced group which were administered with 0.1 ml of CFA intradermally. Group III rats were administered with 10 mg/kg of SCP-CAR nanoparticle composites and group IV rats were given diclofenac sodium (5 mg/kg/day). On the first day of the experiment, excluding the control animals, all the animals present in other groups were given injection of 0.1 ml of Complete Freund's adjuvant (CFA) into the right hind footpad. After completion of the experiment, the rats were anaesthetized and the organs were removed, washed and weighed. Samples from blood and tissues were collected and kept for biochemical, molecular and histopathological study.

2.6. Assessment of body weight and volume of hind paw

Body weight and volume of hind paw of experimental animals were measured from the 1st day of the experiment till the completion of experimental period (25th day). Difference between body weight and hind paw volume of experimental animals was assessed by deducting final body weight and hind paw volume from the initial weight and volume (Lee et al., 2009).

2.7. Measurement of organ weight

After the completion of the experiment, spleen and thymus was removed from the animals and weighed (Hu et al., 2005). Organ weight was represented as the organ weight ratio versus body weight of animals in respective groups (Zhang et al., 2013).

2.8. Evaluation of arthritis score

Arthritis score in CFA induced animals was examined to assess the severity of the disease and grading. It is represented as 5-point scoring system. Highest arthritic score for animals induced with CFA is score 8 (Paval et al., 2009).

2.9. Measurement of biochemical parameters

Serum was separated from the blood samples obtained from experimental animals and the estimation of alkaline phosphatase (ALP), serum glutamic oxaloacetic transaminase (SGOT) and serum glutamic pyruvic transaminase (SGPT) were performed. All the biochemical estimations were performed using standard procedures (Mythilypriya et al., 2008).

2.10. Measurement of lymphocyte proliferation

The spleen which was removed after sacrifice from the experimental animals was cut into pieces and homogenized in Roswell park memorial park (RPMI) medium. Then the homogenate was filtered and the suspension obtained was centrifuged for 10 min at 2000 rpm. Then about 5 ml of buffer containing potassium bicarbonate, Ethylenediaminetetraacetic acid (EDTA) and ammonium chloride was added to remove the red blood cells (RBCs) and the cells were loaded in wells (1x 10^6 cells/ml). The spleen cells were maintained in CO_2 chamber for 72 h. Finally 3-(4,5-dimethylthiazol-2-yl)-2,5-dip henyl tetrazolium bromide (MTT) and DMSO were added to the cells. Proliferation index can be calculated from the colour developed which was read at 495 nm.

2.11. Analysis of proinflammatory cytokines

Blood samples of experimental animals were collected and serum was separated from the blood samples (Zheng et al., 2014). Protein expression of proinflammatory cytokines in serum such as TNF-α, IL-6, IL-1β, COX, PGE2 and IL-10 were estimated using standard ELISA assay kits and the level

of these cytokines were measured following protocol of manufacturer.

2.12. Measurement of serum antioxidant and prooxidant activity

Status of oxidative stress markers such as Malondialdehyde (MDA), antioxidants such as superoxide dismutase (SOD), catalase (CAT) and reduced glutathione (GSH) levels in arthritic rats were measured using standard methods (Devasagayam and Tarachand, 1987; Marklund and Marklund, 1974; Sinha, 1972; Moron et al., 1979).

2.13. Histological analysis

Hind limb of CFA induced arthritic rats were engrossed in 10% formalin solution for 24 h and then in 5% formic acid. Tissues thus immersed were processed, cut into sections of 5 μm thickness. Then the tissue sections were stained using hematoxylin and eosin and observed using microscope to examine the histological abnormalities of arthritic animals (Patil et al., 2012).

2.14. Statistical analysis

Results obtained from the present study were represented as mean ± standard deviation (SD) (n = 6) and then studied using one-way analysis of variance (ANOVA). Experiment was carried out in triplicates with six animals in each group. '#' represents statistical significance at $p < 0.05$ compared to control and '*' represents statistical significance at $p < 0.05$ compared to arthritis induced group as shown in tables and figures.

3. Results

3.1. XRD patterns of SCP-CAR nanocomposites

XRD patterns of SCP-CAR nanocomposites are shown in Fig. 1A. The typical XRD diffraction peaks are observed at 2θ = 26.38° (110), 33.66° (101), 37.71° (200), 51.56° (211), 54.75° (220), 57.68° (002), 61.67° (310), 64.55° (112), 65.90° (301), 71.15° (202) and 78.64° (321) respectively, which is confirmed of tetragonal structure arrangement of synthesized SCP-CAR nanocomposites.

3.2. Particle size distribution and FESEM images of SCP-CAR nanocomposites

The particle size distribution analysis was identified by using the DLS technique, using an aqueous solution. The sizes of the SCP-CAR nanocomposite were observed at ~157.10 nm (Fig. 1B). The lower and higher magnification of FESEM images of SCP-CAR nanocomposite are shown in Fig. 2 (a–b). The SCP-CAR nanocomposite is formed a spherical structure and the mean particle size was calculated as 73 ± 3 nm for SCP-CAR nanocomposite. Energy Dispersive X-ray analysis (EDX) of the sample SCP-CAR nanocomposite (Fig. 2(c)) shows the elemental composition, the atomic percentages were observed at 4.74% of Sn and 41.00% of O, 39.89% of C, and 14.38% of N in the SCP-CAR nanocomposites.

3.3. UV–Vis absorption spectra analysis of SCP-CAR nanoparticle composites

The optical properties of the prepared SCP-CAR nanocomposite samples, UV–Vis absorption spectrum was recorded in the incident photon wavelength of 200 nm to 1100 nm, which is the electrons absorb light in UV or visible region results in electronic transitions. The absorbance edge peak is observed at 271 nm for SCP-CAR nanocomposites (Fig. 3A).

3.4. FT-IR analysis on SCP-CAR nanocomposites

The synthesized SCP-CAR nanocomposite was confirmed by the FT-IR spectral technique, as shown in Fig. 3B. The wide O—H stretching is observed at 3425 cm^{-1}, symmetric C—H stretching vibration is found to 2924 cm^{-1}, deformation mode of O—H is located at 1633 cm^{-1}, the Sn—O stretching is observed at 626 cm^{-1} for SCP-CAR nanocomposites.

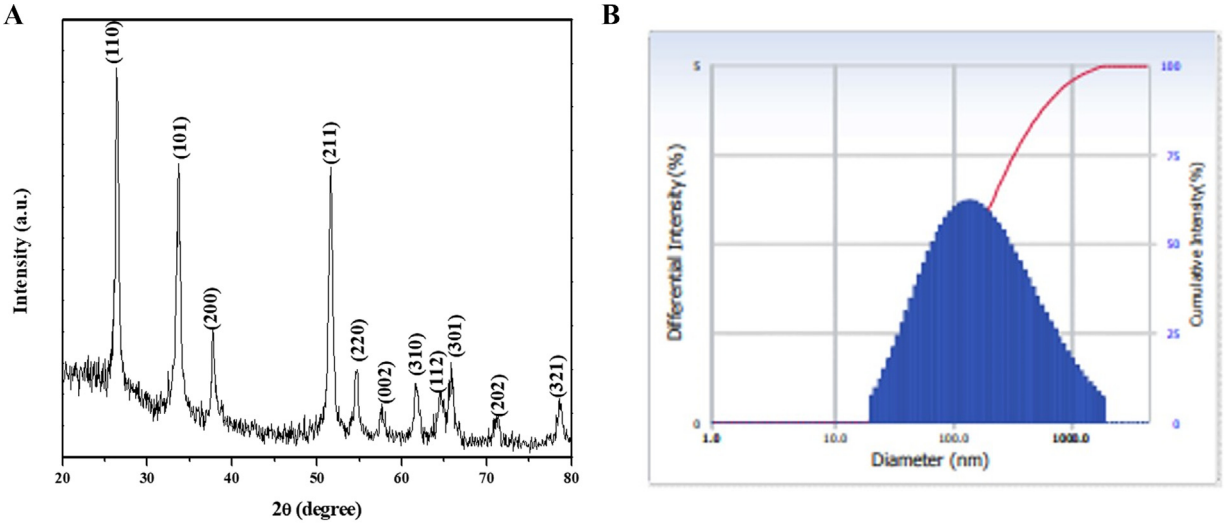

Fig. 1 X-Ray Diffraction pattern and DLS spectrum of SCP-CAR nanocomposites.

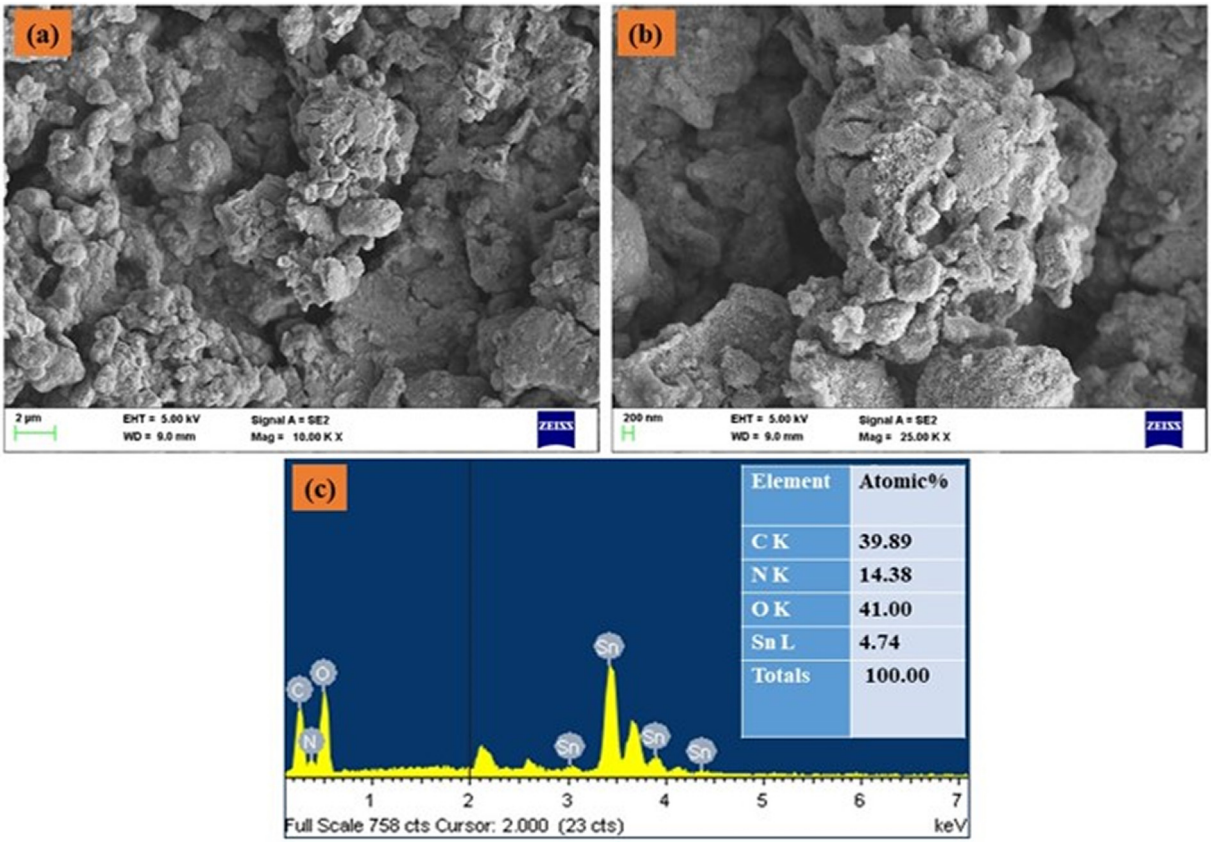

Fig. 2 Lower and higher magnification of FESEM image and EDX spectrum of SCP-CAR nanocomposites.

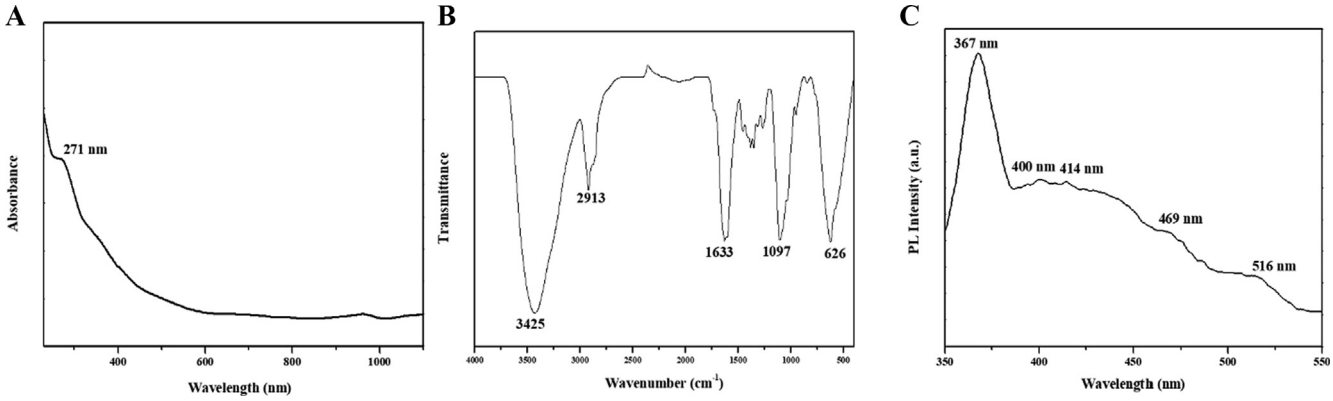

Fig. 3 UV–Vis, FTIR and Photoluminescence spectrum of SCP-CAR nanocomposites.

3.5. Photoluminescence spectrum analysis of SCP-CAR nanocomposites

The photoluminescence spectrum of synthesized SAP-CAR nanocomposite is shown in Fig. 3C which showed an excitation wavelength of 325 nm. The emission spectrum of SAP-CAR nanocomposites, exhibited five peaks, at 367 nm, 400 nm, 414 nm, 469 nm, and 516 nm. The UV peaks at 367 nm, due to the recombination of electron-hole pairs in oxygen and Sn vacancies. The violet emission is observed at 400 nm and 414 nm, which is attributed to the recombination of the CB electron to the V2 + o. The blue emission at 469 nm is corresponding to the electron transition between the V + o to V2 + o.

3.6. Effect of SCP-CAR nanoparticle composite on body weight and organ indices of CFA induced arthritic rats

As represented in Fig. 4, the body weight of animals belonging to arthritis induced group was markedly decreased and the organ index was notably elevated than control group. Administration of SCP-CAR nanoparticle composite (10 mg/kg)

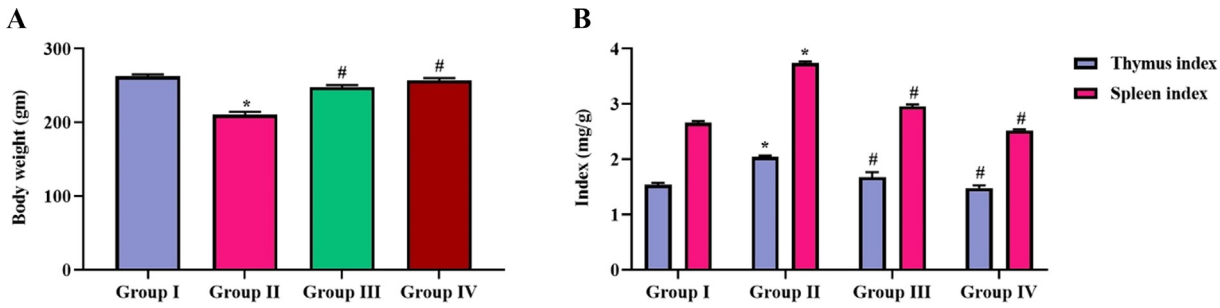

Fig. 4 Effect of SCP-CAR nanoparticle composites on body weight and organ indices of CFA induced arthritic ratsGroup I: Control animals; Group II: Animals induced with arthritis using CFA; Group III: CFA induced arthritic rats + SCP-CAR nanoparticle composites; Group IV: CFA induced arthritic rats + Diclofenac Sodium. Findings of the study were represented as mean ± SD. Experiment was carried out in triplicates consisting of six animals in each group. '#' represents statistical significance at $p < 0.05$ compared to control and '*' represents statistical significance at $p < 0.05$ compared to arthritis induced group.

showed significant increase in body weight while the organ indices were found to diminish than group II animals. Animals administered with standard drug (Group IV) also displayed similar outcome as that of group III animals.

3.7. Effect of SCP-CAR nanoparticle composite on volume of hind paw and arthritis score of CFA induced arthritic rats

The volume of hind paw and arthritis score was found to increase drastically in arthritis induced rats (Group II) than the control group. Marked augmentation in volume of hind paw and index score of arthritis induced animals were noticed starting from day 5–25th day. Supplementation of 10 mg/kg of SCP-CAR nanoparticle composite displayed marked decline in volume of hind paw and arthritis index score in animals induced with arthritis (Group III) (Fig. 5). Diclofenac sodium administration to CFA-challenged rats reduced the volume of hind paw and arthritis index. The reduction of volume of hind paw and arthritis index score brought about by treatment with SCP-CAR nanoparticle composite and diclofenac sodium displayed similar outcomes.

3.8. Effect of SCP-CAR nanoparticle composites on hematological parameters of CFA induced arthritic rats

Level of RBCs and hemoglobin (Hb) was found to decrease significantly and level of white blood cells (WBCs) was increased in arthritic rats when compared to control (Table 1). Arthritis induced rats when supplemented with SCP-CAR nanoparticle composite displayed reversal of hematological parameters such as improved level of RBCs and Hb together with decline in WBCs which is in correlation with animals which are treated with standard drug diclofenac sodium.

3.9. Effect of SCP-CAR nanoparticle composite on marker enzymes of liver function in CFA induced arthritic rats

Fig. 6A exhibited the proliferation of spleen cells index which was markedly increased in CFA-challenged arthritic rats in comparison to control. Remarkable decline in proliferation index of spleen cells were observed in animals treated with SCP-CAR nanoparticle composite (10 mg/kg). Treatment of

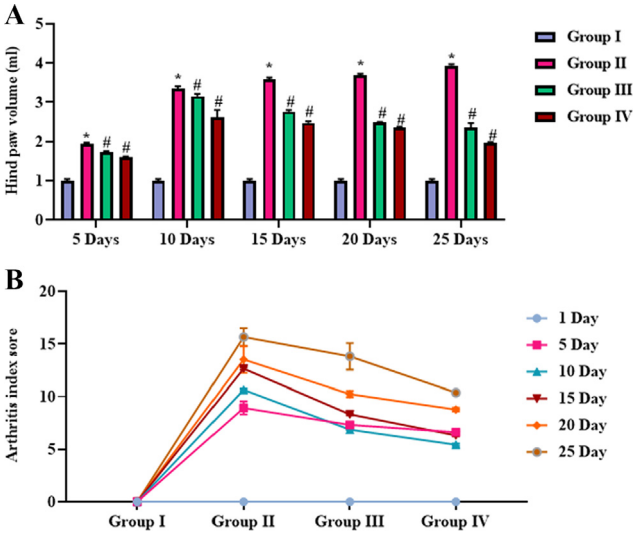

Fig. 5 Effect of SCP-CAR nanoparticle composites on volume of hind paw and arthritis score of CFA induced arthritic rat Group I: Control animals; Group II: Animals induced with arthritis using CFA; Group III: CFA induced arthritic rats + SCP-CAR nanoparticle composites; Group IV: CFA induced arthritic rats + Diclofenac Sodium. Findings of the study were represented as mean ± SD. Experiment was carried out in triplicates consisting of six animals in each group. '#' represents statistical significance at $p < 0.05$ compared to control and '*' represents statistical significance at $p < 0.05$ compared to arthritis induced group.

arthritic rats with diclofenac sodium resulted in similar decline of spleen cell proliferation index comparable to that of group III and control animals.

CFA-induced arthritic rats exhibited considerable rise in level of liver function enzymes such as SGOT, SGPT and ALP compared to control (Fig. 6B). A marked decrease in liver function enzymes were noticed in arthritic rats supplemented with 10 mg/kg of SCP-CAR nanoparticle composite. Arthritis rats administered with diclofenac sodium also displayed reduction in activities of SGOT, SGPT and ALP which is comparable to group III and group I animals.

Table.1 Effect of SCP-CAR nanoparticle composites on hematological parameters of rats induced with arthritis using CFA.

Groups	RBC ($\times 10^6$/µl)	WBC ($\times 10^3$/µl)	Hb (g/dl)
Group I	12.79 ± 5.47	13.49 ± 6.01	13.60 ± 6.29
Group II	4.19 ± 0.82*	21.58 ± 14.98*	5.36 ± 2.38*
Group III	6.68 ± 1.61#	15.5 ± 9.47#	10.17 ± 4.11#
Group IV	9.09 ± 3.49#	14.63 ± 8.25#	12.55 ± 5.47#

Group I: Control animals; Group II: Animals induced with arthritis using CFA; Group III: CFA induced arthritic rats + SCP-CAR nanoparticle composites; Group IV: CFA induced arthritic rats + Diclofenac Sodium. Findings of the study were represented as mean ± SD. Experiment was carried out in triplicates consisting of six animals in each group. '#' represents statistical significance at $p < 0.05$ compared to control and '*' represents statistical significance at $p < 0.05$ compared to arthritis induced group. Note: RBC: Red Blood Cell, WBC: White Blood Cell, Hb: Hemoglobin.

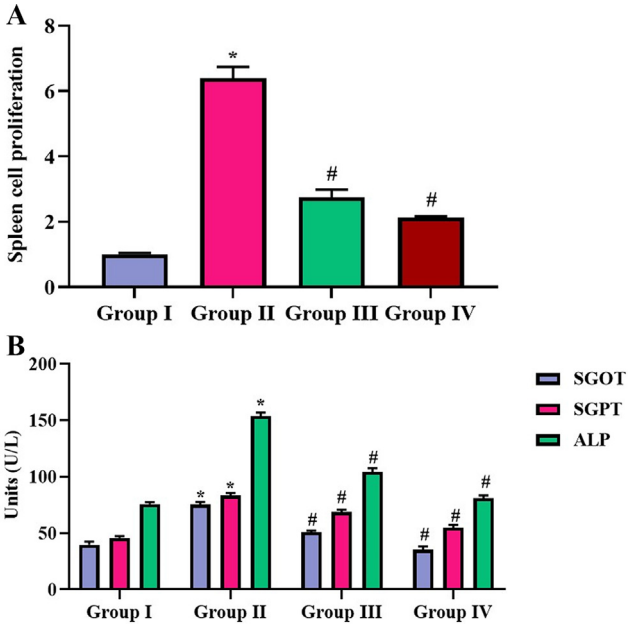

Fig. 6 Effect of SCP-CAR nanoparticle composites on marker enzymes of liver function in CFA induced arthritic rats Group I: Control animals; Group II: Animals induced with arthritis using CFA; Group III: CFA induced arthritic rats + SCP-CAR nanoparticle composites; Group IV: CFA induced arthritic rats + Diclofenac Sodium. Findings of the study were represented as mean ± SD. Experiment was carried out in triplicates consisting of six animals in each group. '#' represents statistical significance at $p < 0.05$ compared to control and '*' represents statistical significance at $p < 0.05$ compared to arthritis induced group.

3.10. Effect of SCP-CAR nanoparticle composite on levels of inflammatory markers in CFA induced arthritic rats

Expression of IL-6, TNF-α, IL-1β, COX-2 and PGE-2 were found to be increased, whereas the level of IL-10 anti-inflammatory marker was found to be lowered in CFA-challenged arthritic rats (Fig. 7 and Fig. 8). Notably, treatment with SCP-CAR nanoparticle composite (10 mg/kg) showed reduction in status of inflammatory markers and resulted in increase in level of IL-10 in arthritis stimulated rats. Standard drug, diclofenac sodium also brough significant reduction in levels of inflammatory mediators and augmented the status of anti-inflammatory marker, IL-10 in rats induced with CFA.

3.11. Effect of SCP-CAR nanoparticle composite on oxidative stress markers in CFA induced arthritic rats

Activities of antioxidant enzymes such as SOD, GSH and CAT were decreased to a marked extent and increase in lipid peroxidation status was observed in animals induced with arthritis (Fig. 9). Following supplementation with 10 mg/kg of SCP-CAR nanoparticle composite to arthritic rats showed decrease in lipid peroxidation and augmented the activities of SOD, CAT and GSH (Group III). Diclofenac sodium treatment to CFA-induced arthritic rats also displayed similar results comparable with animals treated with SCP-CAR nanoparticle composites and control animals.

3.12. Effect of SCP-CAR nanoparticle composite on histopathological analysis of hind paw of CFA induced arthritic rats

Examination of histopathological sections of hind paw of experimental animals was depicted in Fig. 10. CFA-induced arthritic rats (Group II) showed unique signs of hyperplasia in synovial joints, inflammatory cell proliferation, development of pannus and joint and cartilage destruction in contrast to control. SCP-CAR nanoparticle composite supplementation to arthritis induced rats portrayed reduction in inflammatory cell proliferation and the destruction of joints were also found to be reduced than group II animals. Arthritis stimulated animals upon treatment with diclofenac sodium, also offered sig-

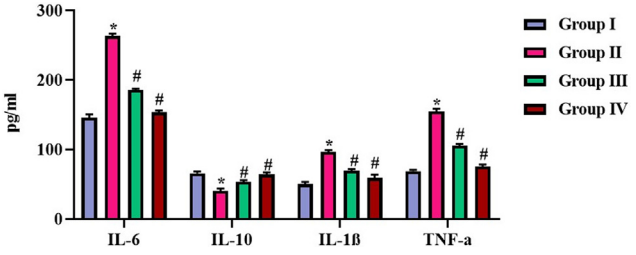

Fig. 7 Effect of SCP-CAR nanoparticle composites on levels of IL-6, IL-10, IL-1β and TNFα in CFA induced arthritic rats Group I: Control animals; Group II: Animals induced with arthritis using CFA; Group III: CFA induced arthritic rats + SCP-CAR nanoparticle composites; Group IV: CFA induced arthritic rats + Diclofenac Sodium. Findings of the study were represented as mean ± SD. Experiment was carried out in triplicates consisting of six animals in each group. '#' represents statistical significance at $p < 0.05$ compared to control and '*' represents statistical significance at $p < 0.05$ compared to arthritis induced group.

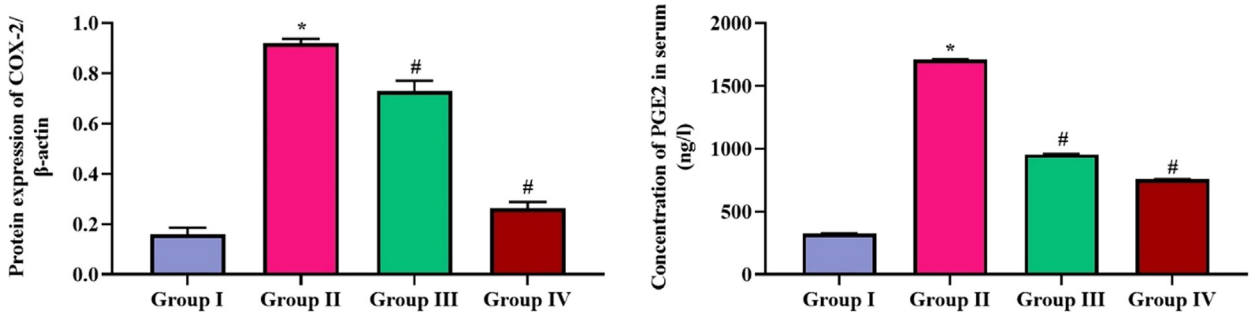

Fig. 8 Effect of SCP-CAR nanoparticle composites on serum levels of cox-2/PGE2 in rats induced with arthritis using CFA Group I: Control animals; Group II: Animals induced with arthritis using CFA; Group III: CFA induced arthritic rats + SCP-CAR nanoparticle composites; Group IV: CFA induced arthritic rats + Diclofenac Sodium. Findings of the study were represented as mean ± SD. Experiment was carried out in triplicates consisting of six animals in each group. '#' represents statistical significance at $p < 0.05$ compared to control and '*' represents statistical significance at $p < 0.05$ compared to arthritis induced group.

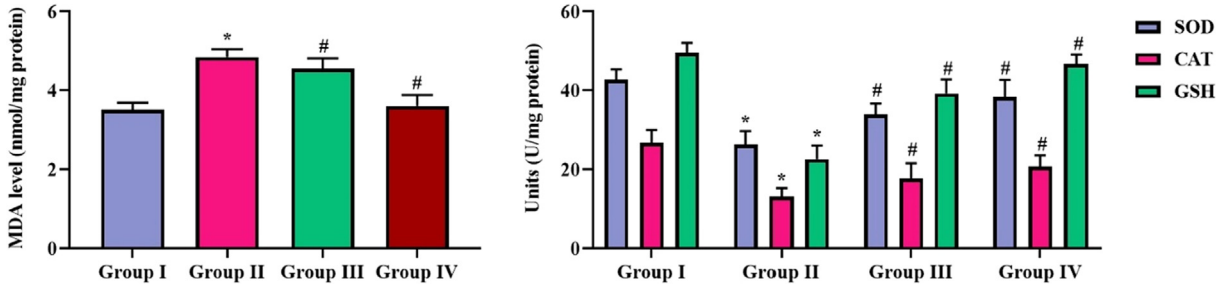

Fig. 9 Effect of SCP-CAR nanoparticle composites on status of oxidative stress markers in CFA induced arthritic rats Group I: Control animals; Group II: Animals induced with arthritis using CFA; Group III: CFA induced arthritic rats + SCP-CAR nanoparticle composites; Group IV: CFA induced arthritic rats + Diclofenac Sodium. Findings of the study were represented as mean ± SD. Experiment was carried out in triplicates consisting of six animals in each group. '#' represents statistical significance at $p < 0.05$ compared to control and '*' represents statistical significance at $p < 0.05$ compared to arthritis induced group. MDA: Malondialdehyde.

nificant protection to bone joints and cartilages which is similar to changes observed in group III and control animals.

4. Discussion

RA, being the most common form of auto-immune disease that influences approximately 1% of the population globally (Shabbir et al., 2016). It is represented by distinguishing features such as joint pain, swelling, joint stiffness and other related clinical complications. Nanoparticles has acquired increased consideration among the investigators because of their explicit therapeutic and pharmacological properties that widens their necessity in areas of biomedical research (Nations et al., 2015).

The typical XRD diffraction peaks are observed at 2θ = 26.38° (110), 33.66° (101), 37.71° (200), 51.56° (211), 54.75° (220), 57.68° (002), 61.67° (310), 64.55° (112), 65.90° (301), 71.15° (202) and 78.64° (321) respectively, which is confirmed of tetragonal structure arrangement of synthesized Tin oxide-Chitosan-Polyethylene glycol- Carvacrol nanocomposites. The resulted from XRD peaks are well-matched with the JCPDS card No. 88-0287, revealed the tetragonal rutile-type SnO2 (space group P42/mnm) crystalline structure. The present work confirms that Chitosan-Polyethylene glycol- Carvacrol molecules have successfully substituted on the SnO2 matrix. The average crystallite size is found at 65 nm calculated using Debye-Scherrer formula $(D) = (0.9\ \lambda)/(\beta \cos\theta)$ (Cullity, 1967). The synthesized SCP-CAR nanocomposite was confirmed by the FT- IR spectral technique. The wide O—H stretching is observed at 3425 cm^{-1}, symmetric C—H stretching vibration is found to 2924 cm^{-1}, deformation mode of O—H is located at 1633 cm^{-1}, the Sn—O stretching is observed at 626 cm^{-1} for SCP—CAR nanocomposites (Tang et al., 2015). Nanoparticle size plays a vital role in changing material properties. UV–Visible spectroscopy is the most widely used method to observe the optical properties of nanoparticles. The optical properties of the prepared SCP-CAR nanocomposite samples was measured using UV–Vis absorption spectrum in the incident photon wavelength of 200 nm to 1100 nm, where the electrons absorb light in UV or visible region that results in electronic transitions (Williams, 2004). The absorbance edge peak is observed at 271 nm for SCP-CAR nanocomposites. Sharp peak of nanoparticle composites represent the monodispersed nature of distribution found in nanoparticles (Zhang et al., 2002).

When the surface state recombines, photoluminescence will be produced, where strong photoluminescence when observed shows very shallow surface states (Chestnoy et al., 1986). The emission spectrum of SAP-CAR nanocomposites, exhibited five peaks, at 367 nm, 400 nm, 414 nm, 469 nm, and 516 nm. The UV peaks at 367 nm, due to the recombination

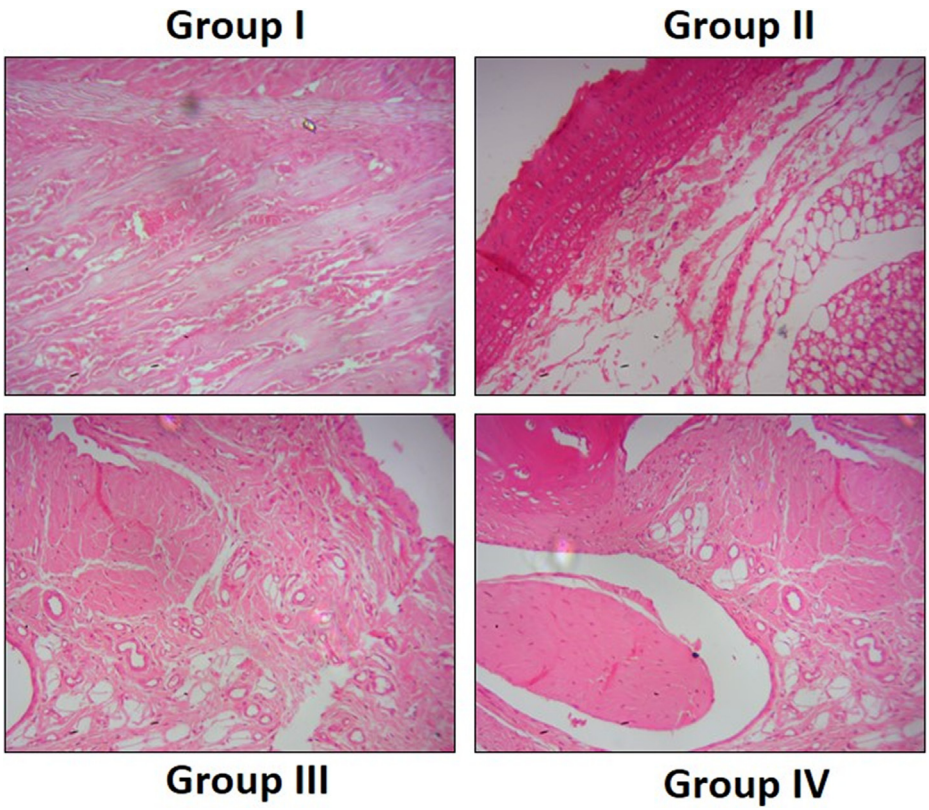

Fig. 10 Effect of SCP-CAR nanoparticle composites on histopathological investigation of hind paw of CFA induced arthritic rats (Magnification x400) Group I: Control animals; Group II: Animals induced with arthritis using CFA; Group III: CFA induced arthritic rats + SCP-CAR nanoparticle composites; Group IV: CFA induced arthritic rats + Diclofenac Sodium.

of electron-hole pairs in oxygen and Sn vacancies. The violet emission is observed at 400 nm and 414 nm, which is attributed to the recombination of the CB electron to the V2 + o. The blue emission at 469 nm, is corresponding to the electron transition between the V + o to V2 + o (Yang et al., 2014). The green emission is located at 516 nm, which may be the interactions between these oxygen and interfacial tin vacancies.

Results obtained also showed that the SCP-CAR nanoparticle composites showed potent anti-arthritic action against RA in rats induced with CFA. Chitosan and its derivatives present in nanoparticle composites was reported to have potent antioxidant and anti-arthritic action in osteoarthritis induced model of rabbit. The findings observed from earlier literature evidences showed that the animals induced with RA displayed similar pathological and immunological response that is comparable to that of RA in humans.

Chronic inflammation and severity of disease progression might have brought about reduction in bodyweight of animals induced with RA using CFA (Kong et al., 2013). Administration of herbal compounds was found to increase the body weight of animals. In present investigation also the reduction in body weight observed in animals induced RA was reversed on administration with 10 mg/kg of SCP-CAR nanoparticle composites. Clinical signs observed in experimental animals induced with RA showed chronic inflammation, joint pain, swelling and joint deformity which is similar to outcomes reported in humans suffering from RA. (Zheng et al., 2014). Swelling, joint pain and edema observed in hind paw of experimental animals following intradermal injection of CFA might have resulted in chronic process of inflammation. Progression of RA in animals can be noticed by joint swelling. Odema arising in CFA-induced arthritic rats is because of increased production of synovial fluids and its vascular infiltration and penetration to cells present in region of inflammation (Alamgeer et al., 2017). In the present study, we observed increased edema and penetration into cells suggestive of chronic inflammation in rats induced with RA. SCP-CAR nanoparticle composites when administered to experimental animals resulted in decrease in volume of paw and arthritis score in CFA-challenged animals. Decrease in inflammatory reactions and secondary lesion progression following SCP-CAR nanoparticle composites administration to rats induced with RA depicts the anti-inflammatory and anti-arthritic potency of nanoparticle composites.

Principal modulators for initiation and progression of RA include pro-inflammatory cytokines, monocytes, lymphocytes and synovial cells. Pathological processes that take place during RA progression are mediated by potent pro-inflammatory mediators such as TNF-α, IL-6 and IL-1 (Cheng et al., 2015). Status of pro-inflammatory modulators was altered in arthritic rats induced by CFA. Significant upregulation in the levels of these pro-inflammatory mediators are considered to be responsible for the pathological mechanisms that involve progression of arthritis (Kim and Moudgil, 2017). Deformities in bones and cartilages, oxidative injury and state of chronic inflammation exaggerate the disease progression resulting in marked

raise in the levels of IL-6, TNF-α and COX-2 in joint tissues. Enhanced production of such proinflammatory modulators triggers the expression of markers of oxidative stress, stimulates inflammatory reactions and promotes injuries in response to oxidative stress (Xie et al., 2015).

Increased accumulation of TNF-α was reported to aggravate the expression of PGE2, IL-1β and IL-6 and results in hyperplasia of synovial joints, increase the accumulation of enzymes causing destruction, activates collagenase and results in deformities of osteoclast that contributes to arthritic decay (Alumno et al., 2017). IL-6 was reported to increase resorption of bones, immunological responses and stimulate accumulation of auto-antibodies. IL-1β increases the osteoclast stimulation and promotes accumulation of degrading enzymes resulting in damage to bones. Upregulated PGE-2 level was closely associated with joint swelling, redness, pain, dilatation of blood vessels and corrosion of cartilage (McCoy et al., 2002). Likewise, the therapeutic drugs reported with anti-arthritic effect must hinder the pro-inflammatory modulators expression in order to lessen severity of arthritis. Thus, the findings of the present study also showed that the nanoparticle composites when administered to arthritic induced rats showed remarkable decrease in level of anti-inflammatory modulators.

Biochemical and hematological parameters were also studied in experimental groups. Animals which were administered with CFA were found to show marked decrease in status of Hb and RBCs. Low level of RBCs represent anaemic condition which has resulted from decreased erythropoietin production, destruction and reduction in functions of RBCs, reduced function of bone marrow and decreased iron content. All these events finally results in stimulation of inflammatory mediator such as IL-1. Increase in content of WBCs observed in CFA-induced arthritic rats might have brought about the immune system activation against destruction causing pathogens thus resulting in activation of inflammatory modulators (Kim et al., 2016). Hematological abnormalities observed in CFA-challenged animals, such as increased WBCs and reduction in content of RBCs and Hb represent the RA severity (Liu and Wang, 2014). In the present findings also we observed noticeable decrease in RBCs and Hb levels, whereas WBCs were elevated to a remarkable extent in CFA-induced arthritic rats. Supplementation of nanoparticle composites to arthritis induced animals resulted in increase in RBCs and Hb and decreased WBCs status.

Cellular oxidative injury results from enhanced levels of lipid peroxides, increased production of ROS, PGE-2 and COX-2 that are considered as crucial mediators for causing oxidative injuries. GSH acts as an antioxidant defense to protect from cellular oxidative stress. Besides the protective action of antioxidant enzymes, enhanced ROS generation, upregulated expression of COX-2 and PGE2 results in loss of homeostatic balance between enzymic and non-enzymic antioxidants that destroys antioxidant defense functions. Such condition also reduces the activity of SOD that causes detoxification of peroxide and superoxide radicals and CAT involved in hydrogen peroxide detoxication (Comar et al., 2013). Earlier literature evidences suggests that increased accumulation of reactive oxygen species and free radicals promotes the pathological processes involved in RA. Such increase in ROS production and free radical generation in RA results in reduction of antioxidant enzyme activities which further aggravates RA progression resulting in necrosis of cells and increased oxidative stress (Shi et al., 2015). Status of antioxidant enzymes such as SOD, CAT and GSH were upregulated and decline in status of lipid peroxidation was observed in arthritis induced rats supplemented with NPs which confirms the antioxidant activity of SCP-CAR nanoparticle composites.

Noticeable increase in levels of liver function markers such as SGPT, SGOT and ALP were observed in serum of CFA-induced experimental animals. Marked increase in liver specific enzymes particularly during RA progression is correlated with chronic injuries to bones (Xu et al., 2017). Decrease activity of SGOT, ALP and SGPT was observed in RA induced rats supplemented with SCP-CAR nanocomposites. Together the findings of the present investigation exhibited potent anti-arthritic and anti-inflammatory potency of SCP-CAR nanocomposites against RA.

5. Conclusion

SCP-CAR nanocomposites displayed potent anti-arthritic and anti-inflammatory action against rats induced with RA. Arthritic animals when administered with nanoparticle composites portrayed remarkable protection against CFA-induction via its anti-inflammatory and anti-arthritic ability. SCP-CAR nanoparticle composites showed augmented status of antioxidants, reduced the levels of pro-inflammatory modulators, altered histological abnormalities and bone destruction in rats administered with CFA. Hence, it can concluded that SCP-CAR nanoparticle composites can be used likely as a therapeutic agent to treat against RA. Besides these findings, further additional investigations should be accomplished in future to understand the mechanism through which the nanoparticle composites can act against CFA-induced arthritic animals.

Declaration of Competing Interest

The authors declare that they have no known competing financial interests or personal relationships that could have appeared to influence the work reported in this paper.

Acknowledgement

This project was supported by Researchers Supporting Project number (RSP-2021/230) King Saud University, Riyadh, Saudi Arabia.

References

Alamgeer, Uttra, A.M., Hasan, U.H., 2017. Anti-arthritic activity of aqueous-methanolic extract and various fractions of BerberisorthobotrysBien ex Aitch. BMC Complement. Altern. Med. 17, 371.

Alumno, A., Carubbi, F., Giacomelli, R., Gerli, R., 2017. Cytokines in the pathogenesis of rheumatoid arthritis: new players and therapeutic targets. BMC. Rheumatol. 1, 3.

Baranauskaite, J. et al, 2017. The influence of different oregano species on the antioxidant activity determined using HPLC postcolumn DPPH method and anticancer activity of carvacrol and rosmarinic acid. Biomed. Res. Int. 2017, 1681392.

Barnwal, P. et al, 2017. Benzo(a)pyrene induces lung toxicity and inflammation in mice: prevention by carvacrol. Hum Exp Toxicol. 37, 752–761.

Bihani, G.V., Rojatkar, S.R., Bodhankar, S.L., 2014. Anti-arthritic activity of methanol extract of Cyathoclinepurpurea (whole plant) in Freund's complete adjuvant-induced arthritis in rats. Biomed. Aging Pathol. 4, 197–206.

Cheng, X.L., Liu, X.G., Wang, Q., Zhou, L., Qi, L.W., Li, P., Liu, E. H., 2015. Anti-inflammatory and anti-arthritic effects of GugeFengtong Formula: in vitro and in vivo studies. Chin J. Nat. Med. 13, 842–853.

Chestnoy, N., Harris, T.D., Hull, R., Brus, L.E., 1986. Luminescence and photophysics of CdS semiconductor clusters: the nature of the emitting electronic state. J. Phys. Chem. 90 (15), 3393–3399.

Comar, J.F., Babeto de Sa-Nakanishi, A., de Oliveira, A.L., Marques Nogueira Wendt, M., Bersani Amado, C.A., Ishii Iwamoto, E.L., Peralta, R.M., Bracht, A., 2013. Oxidative state of the liver of rats with adjuvant-induced arthritis. Free Radic. Biol. Med. 58, 144–153.

Cullity, B.D., 1967. Elements of X-Ray Diffraction. Addison-Wesley, Reading, Mass, USA.

Dai, W., Qi, C., Wang, S., 2018. Synergistic effect of glucosamine and vitamin E against experimental rheumatoid arthritis in neonatal rats. Biomed. Pharmacother. 105, 835–840.

Devasagayam, T.P., Tarachand, U., 1987. Decreased lipid peroxidation in the rat kidney during gestation. Biochem. Biophys. Res. Commun. 145, 134–138.

El-Gaphar, O.A.M.A., Abo-Youssef, A.M., Abo-Saif, A.A., 2018. Effect of losartan in complete freund's adjuvant –induced arthritis in rats. Iranian J. Pharmaceut. Res. 17, 1420–1430.

Furst, D.E., Emery, P., 2014. Rheumatoid arthritis pathophysiology: update on emerging cytokine and cytokine-associated cell targets. Rheumatol. 53, 1560–1569.

Grygielska, J., Raciborski, F., Kłak, A., Owoc, J., 2018. The impact of nutrition and generally available products such as nicotine and alcohol on rheumatoid arthritis – review of the literature. Reumatolog. 56, 121–127.

Hu, F., Hepburn, R., Li, Y., et al, 2005. Effects of ethanol and water extracts of propolis (bee glue) on acute inflammatory animal models. J. Ethnopharmacol. 100, 276–283.

Kapoor, B., Singh, S.K., Gulati, M., Gupta, R., Vaidya, Y., 2014. Application of liposomes in treatment of rheumatoid arthritis: Quo vadis. Sci. World J. 2014, 978351.

Katwal, R., Kaur, H., Sharma, G., Naushad, M., Pathania, D., 2015. Electrochemical synthesized copper oxide nanoparticles for enhanced photocatalytic and antimicrobial activity. J. Ind. Eng. Chem. 31, 173–184.

Khashan, K.S., Sulaiman, G.M., Abdulameer, F.A., 2016. Synthesis and antibacterial activity of CuO nanoparticles suspension induced by laser ablation in liquid. Arab. J. Sci. Eng. 41, 301–310.

Kim, E.Y., Moudgil, K.D., 2017. Immunomodulation of autoimmune arthritis by pro-inflammatory cytokines. Cytokine 98, 87–96.

Kim, W., Park, S., Choi, C., Kim, Y.R., Park, I., Seo, C., Youn, D., Shin, W., Lee, Y., Choi, D., Kim, M., Lee, H., Kim, S., Na, C., 2016. Evaluation of anti-inflammatory potential of the new Ganghwaljetongyeum on adjuvant-induced inflammatory arthritis in rats. Evid. Compl. Alternat. Med., 1230294

Kong, X., Liu, C., Zhang, C., Zhao, J., Wang, J., Wan, H., Zhu, H., Zhang, P., Chen, W., Xiao, Y., Lin, N., 2013. The suppressive effects of Saposhnikoviadivaricata(Fangfeng) chromone extract on rheumatoid arthritis via inhibition of nuclear factor-jB and mitogen activated proteinkinases activation on collagen-induced arthritis model. J. Ethnopharmacol. 148 (3), 842–850.

Kumar, M., Muzzarelli, R.A.A., Muzzarelli, C., et al, 2004. Chitosan chemistry and pharmaceutical perspectives. Chem Rev. 104, 6017–6084.

Lee, D.Y., Choo, B.K., Yoon, T., et al, 2009. Anti-inflammatory effects of Asparagus cochinchinensis extract in acute and chronic cutaneous inflammation. J. Ethnopharmacol. 121, 28–34.

Lee, J.H., Kim, Y.G., Lee, J., 2017. Carvacrol-rich oregano oil and thymol-rich thyme red oil inhibit biofilm formation and the virulence of uropathogenic *Escherichia coli*. J. Appl. Microbiol. 123, 1420–1428.

Liu, H.M., Wang, K.J., 2014. Therapeutic effect of Captopril on rheumatoid arthritis in rats. Asian Pac. J. Trop. Med. 7 (12), 996–999.

Marklund, S., Marklund, G., 1974. Involvement of the superoxide anion radical in the autoxidation of pyrogallol and a convenient assay for superoxide dismutase. Eur. J. Biochem. 47, 469–474.

McCoy, J.M., Wicks, J.R., Audoly, L.P., 2002. The role of prostaglandin E2 receptors in the pathogenesis of rheumatoid arthritis. J. Clin. Invest. 110 (5), 651–658.

McInnes, I.B., Schett, G., 2017. Pathogenetic insights from the treatment of rheumatoid arthritis. The Lancet 389, 2328–2337.

Moron, M.S., Depierre, J.W., Mannervik, B., 1979. Levels of glutathione, glutathione reductase and glutathione S-transferase activities in rat lung and liver. Biochim. Biophys. Acta. 582, 67–78.

Mythilypriya, R., Shanthi, P., Sachdanandam, P., 2008. Salubrious effect of Kalpaamruthaa, a modified indigenous preparation in adjuvant induced arthritis in rats: a biochemical approach. Chem. Biol. Interact. 173, 148–158.

Nations, S., Long, M., Wages, M., Maul, J.D., Theodorakis, C.W., Cobb, G.P., 2015. Subchronic and chronic developmental effects of copper oxide (CuO) nanoparticles on Xenopuslaevis. Chemosphere 2015 (135), 166–174.

Okada, Y., Eyre, S., Suzuki, A., Kochi, Y., Yamamoto, K., 2019. Genetics of rheumatoid arthritis: 2018 status. Ann. Rheumatic Dis. 78, 446–453.

Ong, S.Y., Wu, J., Moochhala, S.M., et al, 2008. Development of a chitosan-based wound dressing with improved hemostatic and antimicrobial properties. Biomaterials 29, 4323–4332.

Pan, T., Cheng, T., Jia, Y., Li, P., Li, F., 2017. Anti-rheumatoid arthritis effects of traditional Chinese herb couple in adjuvant induced arthritis in rats. J. Ethnopharmacol. 205, 1–7.

Patil, M.V.K., Kandhare, A.D., Bhise, S.D., 2012. Anti-arthritic and anti-inflammatory activity of Xanthium srtumarium L. ethanolic extract in Freund's complete adjuvant induced arthritis. Biomed Aging Pathol. 2, 6–15.

Paval, J., Kaitheri, S.K., Potu, B.K., et al, 2009. Anti-arthritic potential of the plant Justicia gendarussa Burm F. Clinics. 64, 357–362.

Pham, C.T., 2011. Nanotherapeutic approaches for the treatment of rheumatoid arthritis. Wiley Interdiscip. Rev. Nanomed. Nanobiotechnol. 3, 607–619.

Ruiz, P., Katsumiti, A., Nieto, J.A., Bori, J., Jimeno-Romero, A., Reip, P., Arostegui, I., Orbea, A., Cajaraville, M.P., 2015. Shortterm effects on antioxidant enzymes and long-term genotoxic and carcinogenic potential of CuO nanoparticles compared to bulk CuO and ionic copper in mussels Mytilusgalloprovincialis. Mar. Environ. Res. 111, 107–120.

Safa, S., Azimirad, R., Moghaddam, S.S., Rabbani, M., 2016. Investigating on photocatalytic performance of CuO micro and nanostructures prepared by different precursors. Desalin. Water Treatment. 57, 6723–6731.

Serra, P., Santamaria, P., 2015. Nanoparticle-based autoimmune disease therapy. Clin. Immunol. 160, 3–13.

Shabbir, A., Shahzad, M., Ali, A., Zia-ur-Rehman, M., 2016. Discovery of new benzothiazine derivative as modulator of proand anti-inflammatory cytokines in rheumatoid arthritis. Inflammation 39 (6), 1918–1929.

Shi, M., Cui, F., Liu, A.J., Ma, H.J., Cheng, M., Song, S.X., Yuan, F., Li, D.P., Zhang, Y., 2015. The protective effects of chronic intermittent hypobaric hypoxia pretreatment against collagen induced arthritis in rats. J. Inflamm. 12, 23.

Singh, D.K., Ray, A.R., 2000. Biomedical applications of chitin, chitosan and their derivates. Rev. Macromol.: Chem. Phys., 69–83

Singh, P. et al, 2016. Reinvestigation of essential oil of *Rabdosia melissoides*: Chemical composition, antioxidant, anti-inflammatory, analgesic, antipyretic, antifungal and antibacterial activities. J. Essent Oil-Bear Plants. 19, 1859–1872.

Sinha, A.K., 1972. Colorimetric assay of catalase. Anal. Biochem. 47, 389–394.

Tang, L., Lee, Y.R., Kim, J., Shim, J.J., 2015. Photocatalytic activity of reduced graphene oxide/SnO2 nanocomposites prepared in ionic liquid. Synthetic Metals 201, 54–60.

Ulbrich, W., Lamprecht, A., 2010. Targeted drug-delivery approaches by nanoparticulate carriers in the therapy of inflammatory diseases. J. R. Soc. Interface 7 (Suppl. 1), S55–S66.

William, T.S., 2004. Laser fundamentals.

Xie, J., Fu, N., Cai, L.Y., Gong, T., Li, G., Peng, Q., Cai, X.X., 2015. The effects of interleukin-1beta in modulating osteoclast-conditioned medium's influence on gelatinases in chondrocytes through mitogen-activated protein kinases. Int. J. Oral Sci. 7, 220–231.

Xu, Q., Zhou, Y., Zhang, R., Sun, Z., Cheng, L., 2017. Antiarthritic activity of qi-wu rheumatism granule (a Chinese herbal compound) on complete freund's adjuvant-induced arthritis in rats. Evid. Based Complement. Altern. Med., 1–13

Yang, J.K., Zhao, H.L., Li, J., Zhao, L.P., Chen, J.J., Yu, B., 2014. Structural and optical properties and photoluminescence mechanism of fluorine-doped SnO2 films during the annealing process. Acta materialia 62, 156–161.

Yang, M., Feng, X., Ding, J., Chang, F., Chen, X., 2017. Nanotherapeutics relieve rheumatoid arthritis. J. Control. Release 252, 108–124.

Zhang, D.H., Xue, Z.Y., Wang, Q.P., 2002. Formation of ZnO nanoparticles by the reaction of zinc metal with aliphatic alcohols. J. Phys. D 35 (21), 2837–2840.

Zhang, Y.Q., Xu, W., Li, H., et al, 2013. Therapeutic effects of total alkaloids of Tripterygium wilfordii Hook f. on collagen-induced arthritis in rats. J. Ethnopharmacol. 145, 699–705.

Zheng, C.J., Zhao, X.X., Ai, H.W., et al, 2014. Therapeutic effects of standardized Vitex negundo seeds extract on complete Freund's adjuvant induced arthritis in rats. Phytomedicine 21, 838–846.